Supporting Information

Cerium-alloyed dendrite-inhibited highly stable anodes for all-solid-state lithium batteries

Xiaomeng Shi,[a] Zhichao Zeng,*[a] Chao Li,[a] Wenshuo Zhang,[a] Zhiqiang Li,[b] Guangrui Zhang,[b] Lele Gao[b] and Yaping Du*[a]

[a] Tianjin Key Lab for Rare Earth Materials and Applications, Center for Rare Earth and Inorganic Functional Materials, Smart Sensing Interdisciplinary Science Center, School of Materials Science and Engineering, National Institute for Advanced Materials, Nankai University, 38 Tongyan Road, Jinnan District, Tianjin 300350, P.R. China

[b] Inner Mongolia Northern Rare Earth Advanced Materials Technology Innovation Co., Ltd., Rare Earth Advanced Materials Technology Innovation Center, No. 8-66 Rare-earth Street, Jiuyuan District, Inner Mongolia, Baotou 014030, P.R. China

*E-mails: ypdu@nankai.edu.cn; zeng@mail.nankai.edu.cn

Supplementary videos:

Video S1. Schematic diagram of the Brinell hardness test.
Video S2. Li-In- and Li-In-Ce-based special solid cells during cycling.
Video S3. Schematic diagrams of Li-In dendrite growth in Li-In- and Li-In-Ce-based solid cells.

Table of contents

METHODS

Synthesis of Li-In and Li-In-RE Alloys

The Li-In alloys were obtained via a repeated cold pressing method. The Li (China Energy Lithium Co., Ltd.) and In (Changsha HAOJIA New Material Co., Ltd.) plates (molar ratio: 3/7) were overlapped and cold pressed repetitiously, and the Li-In alloys were obtained.

The Li-In-Ce alloys were prepared by melting and cold pressing processes. First, the Ce metal and In plate (molar ratios: 5–95, 10–90, and 14–86) were melted at 700 °C for 5 h in a graphite crucible. The obtained Ce-In alloys were cold pressed with Li metal (molar ratio of Li/In: ~ 3/7), and then, the Li-In-Ce alloys were obtained. The Li-In-RE alloys (molar ratio of RE-In: 10–90) were obtained via the same process. RE (Y, La, Ce, Pr, Sm, and Yb) metals were obtained from by Shanghai Titan Scientific Co., Ltd. All the above processes were protected by argon (Ar).

Synthesis of the Solid Electrolyte

Li_3YBr_6 (LYB) was obtained via the vacuum evaporation assisted method reported in our previous work.[1] First, Li_2CO_3 (99.99%, Shanghai Meryer Chem. Technol. Co., Ltd.) and Y_2O_3 (99.999%, Beijing HWRK Chem. Co., Ltd.) (molar ratio, Li/Y = 3/1) powders were weighed and dissolved in HBr (48.0% w.t., Shanghai Aladdin Biochem. Technol. Co., Ltd.) solution by continuous heating and stirring, forming a transparent solution. After that, the excess NH_4Br (99.0%, Shanghai Aladdin Biochem. Technol. Co., Ltd.) sample was added to form a mixed solution, and the solvent was subsequently dried via a heating process. The obtained semisolid precursor was subsequently heated in an Ar atmosphere and under vacuum. Finally, the LYB were obtained after cooling to room temperature (RT).

Materials Characterization

Rigaku diffractometers (MiniFlex600 (Cu Kα), Smart Lab 3kW (Cu Kα)) were used to collect the X-ray diffraction (XRD) patterns of the Li-In and Li-In-RE alloys. The XRD data were further studied by Rietveld refinement with GSAS-EXPGUI.[2] X-ray photoelectron spectroscopy spectra were collected with a Thermo Scientific spectrometer (ESCALAB 250Xi (Al Kα)). Scanning electron microscopy (SEM) (JEOL JSM-7800F, energy dispersion spectrometer, EDS) was selected to observe the samples. All the characterizations were protected by an Ar atmosphere.

Theoretical Calculation

To analyze the adsorption energy of Li on the surfaces of Li-In (220) and In (110) in Li-In and Li-In-Ce alloys, density functional theory calculations were performed via the Vienna Ab initio Simulation Package.[3,4] The correlation energy and electron exchange and were managed via the generalized gradient approximation method.[5] The adsorption energy of Li was considered as follows:

$$E_A = E_1 - (E_2 + E_{Li})$$

where E_A is the adsorption energy of Li, and E_1, E_2, and E_{Li} are the energies of different states (E_1, Li adsorbed system; E_2, no Li adsorbed system; E_{Li}, Li).

Hardness Characterization

For the Brinell hardness (HB) test of the cold pressed Li-In and Li-In-Ce plates, they were transferred to a custom-made mould, and a cemented carbide ball (diameter, 2.0 mm) was placed on the surface of the sample with a constant load (5.0 kg). The indentation diameters were measured from the corresponding SEM images. The HB values can be obtained according to the following equation:[6]

$$\mathrm{HB} = \frac{P}{0.5\pi D(D - \sqrt{D^2 - d^2})}$$

The unit of HB value is kgf mm^{-2}; D is the diameter of the cemented carbide ball (2.0 mm); d is the indentation diameter; and P is the constant load (5.0 kg).

Electrochemical Characterization

Symmetrical solid cells with Li-In or Li-In-RE electrodes were fabricated via a cold pressing process. First, LYB powder (120 mg) was pressed under 200 MPa in a circular mold to form the LYB pellet (diameter: 10 mm), and the Li-In or Li-In-RE plates were pressed (500 MPa) on the double sides of the LYB pellet. In addition, the symmetrical solid cells with small fabricated pressure of electrodes were prepared to analyze the cycled electrode/electrolyte interface. LYB pellet was formed in a mold (500 MPa), and the Li-In or Li-In-Ce plates were pressed (100 MPa) on the LYB pellet. Symmetrical solid cells based on Li-In or Li-In-RE were subsequently obtained. Electrochemical impedance spectroscopy (EIS) tests of these symmetrical cells were conducted on an Autolab PGSTAT302N instrument at RT. The assembled Li-In or Li-In-RE based symmetrical cells were cycled on a LANHE CT2001A battery test system. The *in situ* EIS was conducted on Li-In- and Li-In-Ce-based symmetrical cells when charged/discharged for 10 min and rested for 60 min, and distribution of relaxation times (DRT) analysis was performed via DRT tools in Matlab software.[7]

Li-In/LYB/LTO ($Li_4Ti_5O_{12}$, LTO) and Li-In-Ce/LYB/LTO cells were also prepared via the cold-pressing method. Preparation of the cathode composite powder: A uniform mixture containing LTO (99.0%, Beijing Innochem Science & Technology Co., Ltd.), LYB and Ketjen Black (KB) (Lion Corporation) (weight ratio, 21:72:7) was obtained via a hand grinding process (30 min). After that, LYB (100 mg), cathode composite (10.0 mg) and Li-In or Li-In-Ce plates were pressed together (500 MPa), forming the Li-In/LYB/LTO or Li-In-Ce/LYB/LTO batteries. These obtained solid batteries were sealed in CR2032 coin cell models and cycled at 1.0 C (175 mA g^{-1}, 1.0 V ~ 2.0 V, *vs.* Li/Li^+). All the processes used to fabricate the above cells were conducted in an Ar atmosphere and measured at RT.

***In Situ* Li-In Dendrites Observation**

For the visualization of *in situ* Li-In dendrites, the corresponding special solid cells were fabricated via a cold pressing process. The Li-In or Li-In-Ce material was pressed and cut into a circular plate (diameter, 8 mm) and then cut into two semicircular plates as electrodes. LYB powder (100 mg) was subsequently pressed in a mold (diameter, 10 mm) under 500 MPa, and the two semicircular Li-In or Li-In-Ce plates were placed on one side of the LYB layer (gap: ~ 1.0 mm) and then pressed (100 MPa). Finally, the assembled special solid cell was placed in a customized transparent mold and cycled at 2.0 mA cm^{-2}.

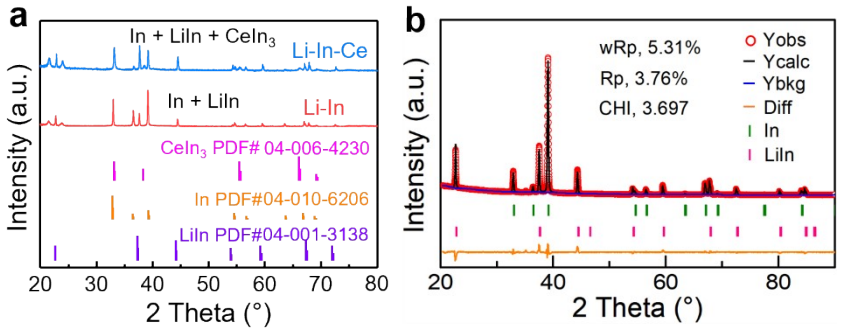

Fig. S1. (a) The XRD results of Li-In and Li-In-Ce alloys. (b) The XRD Rietveld refinement result of Li-In alloy.

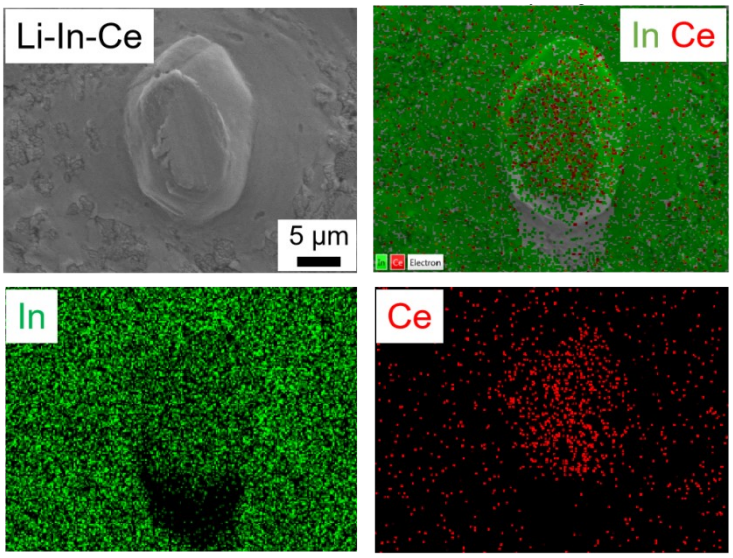

Fig. S2. The SEM image of single particle in Li-In-Ce sample and the corresponding EDS mapping results (In and Ce elements).

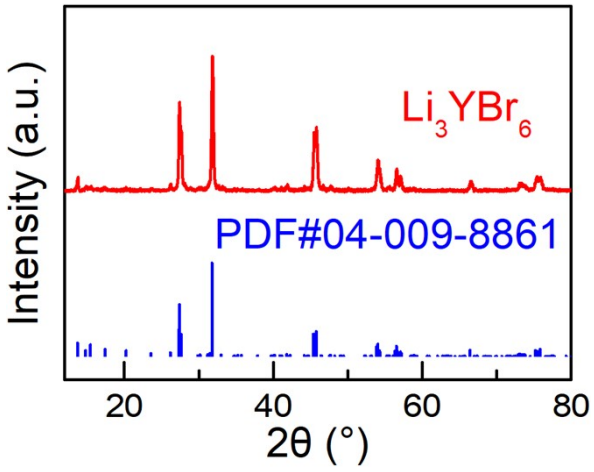

Fig. S3. The XRD pattern of the synthesized Li_3YBr_6 (LYB).

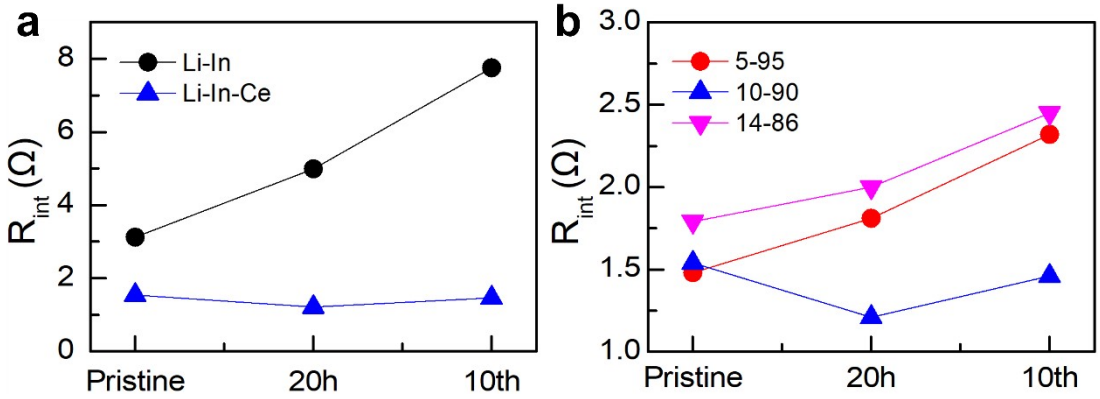

Fig. S4. The interface resistances of the symmetrical solid cells (pristine, rested for 20 h, and after 10 cycles). (a) Li-In and Li-In-Ce (Ce/In = 10/90) act as the electrodes. (b) Li-In-Ce (Ce/In = 5/95, 10/90, and 14/86) act as the electrodes.

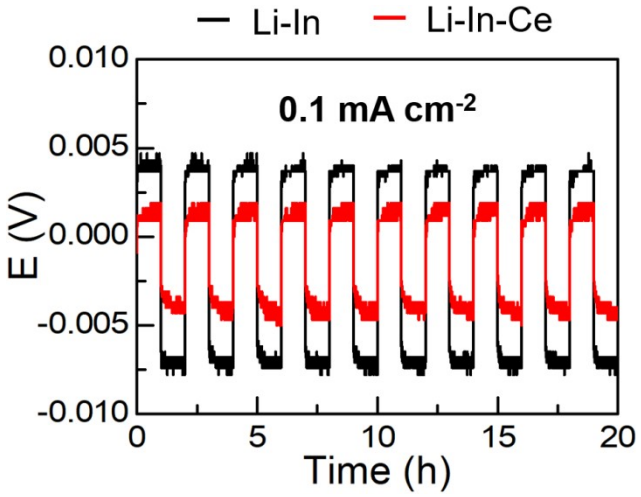

Fig. S5. The voltage-time curves of symmetrical solid cells based on Li-In and Li-In-Ce cycling at 0.1 mA cm^{-2}.

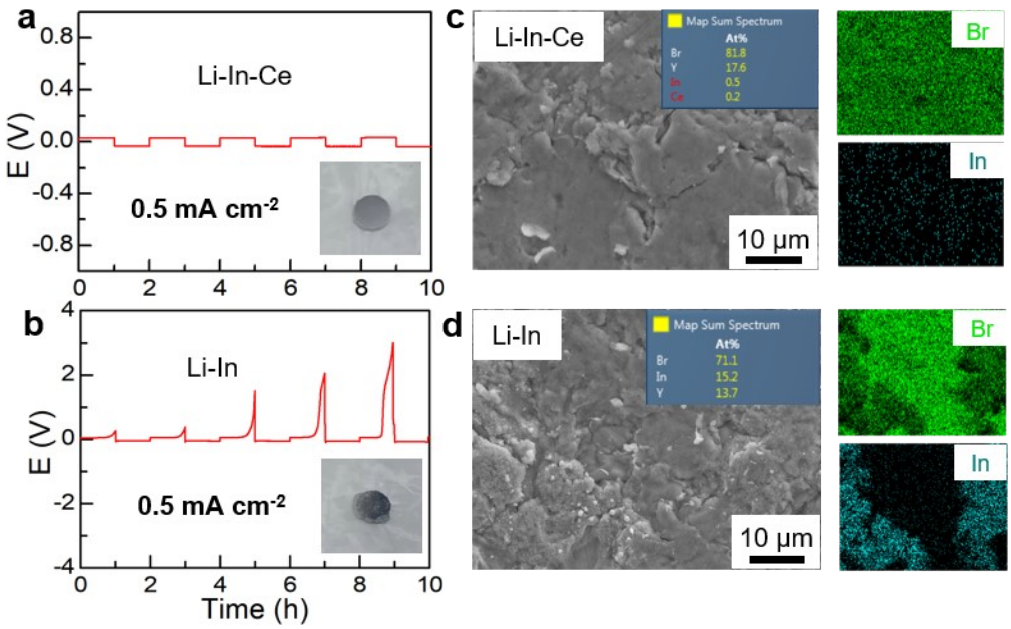

Fig. S6. The voltage-time curves of symmetrical solid cells (5 cycles, 0.5 mA cm^{-2}) based on (a) Li-In-Ce and (b) Li-In. (c, d) The corresponding SEM/EDS and mapping results (In and Br elements) of the cycled LYB layers.

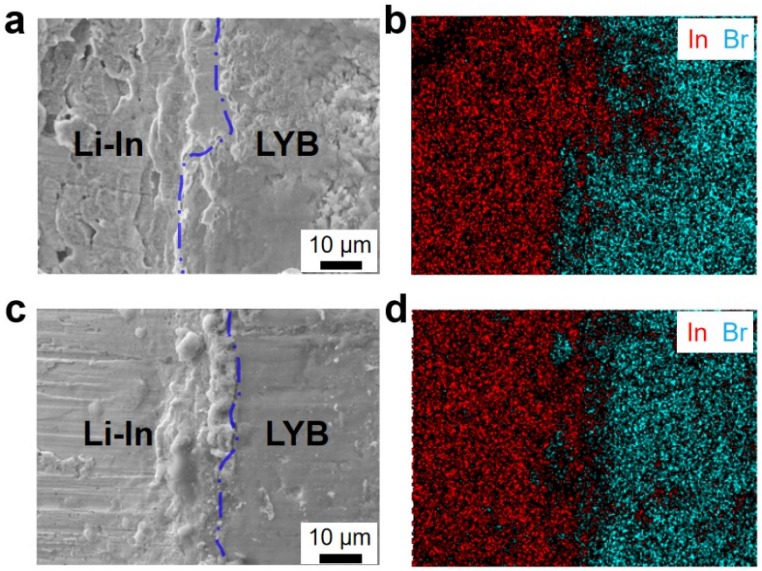

Fig. S7. (a-d) The cross-sectional SEM images and mapping results (In and Br elements) of the pristine and cycled Li-In/LYB layers.

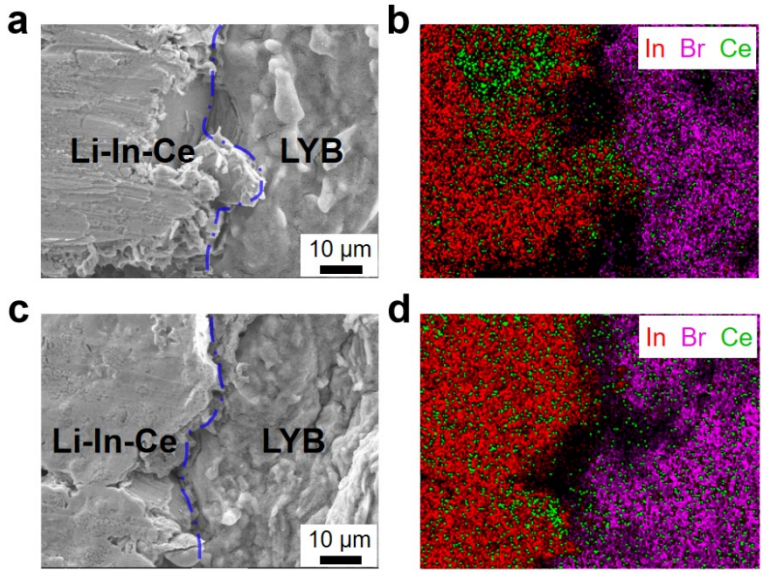

Fig. S8. (a-d) The cross-sectional SEM images and mapping results (In, Br and Ce elements) of the pristine and cycled Li-In-Ce/LYB layers.

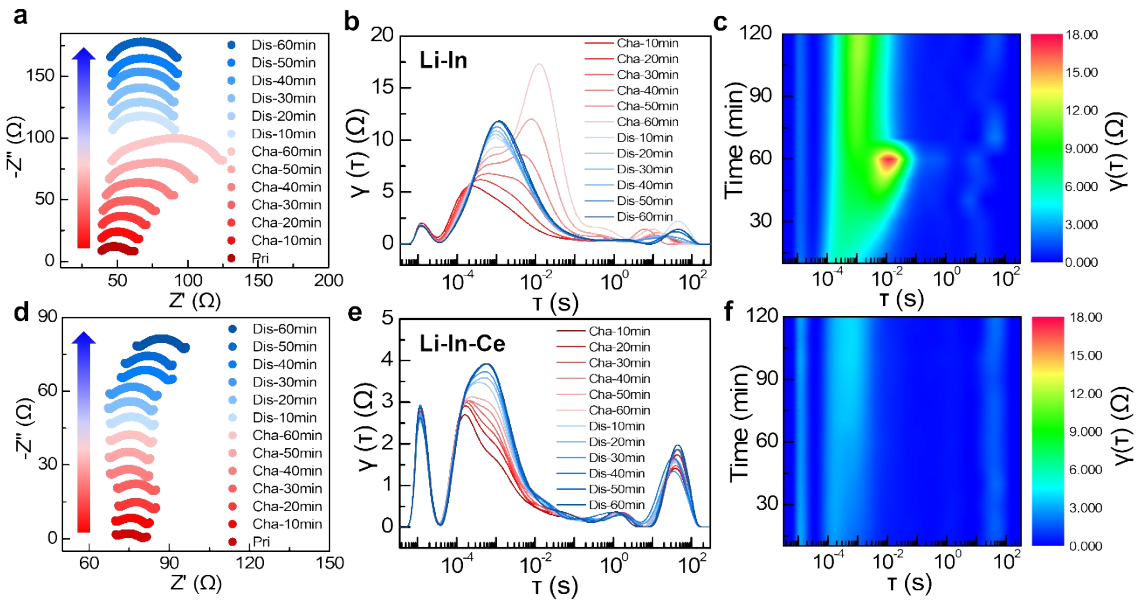

Fig. S9. The *in situ* EIS and DRT results of (a-c) Li-In- and (d-f) Li-In-Ce-based symmetrical cells.

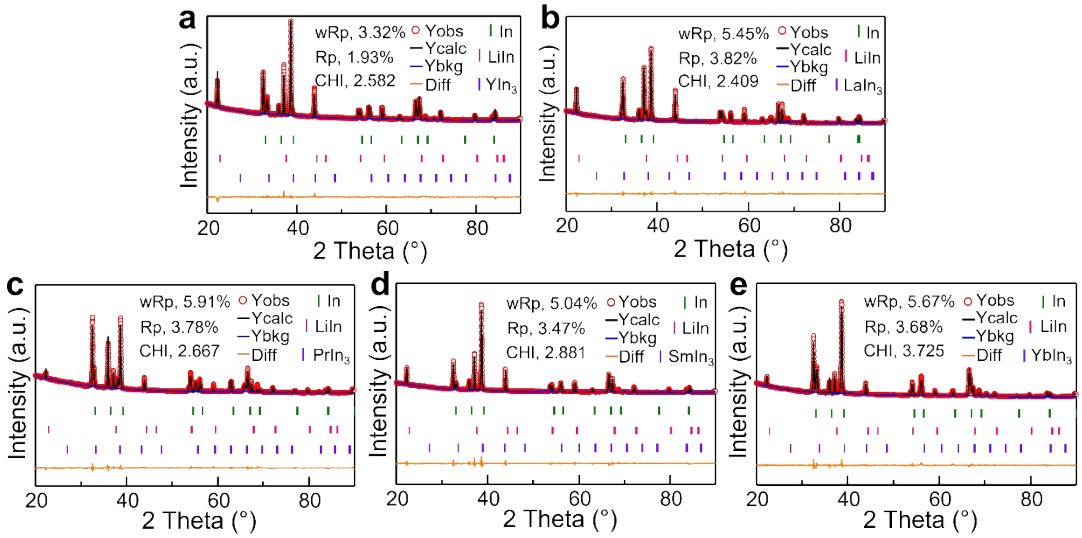

Fig. S10. The XRD Rietveld refinement results of (a-e) Li-In-RE alloys (RE = Y, La, Pr, Sm, or Yb).

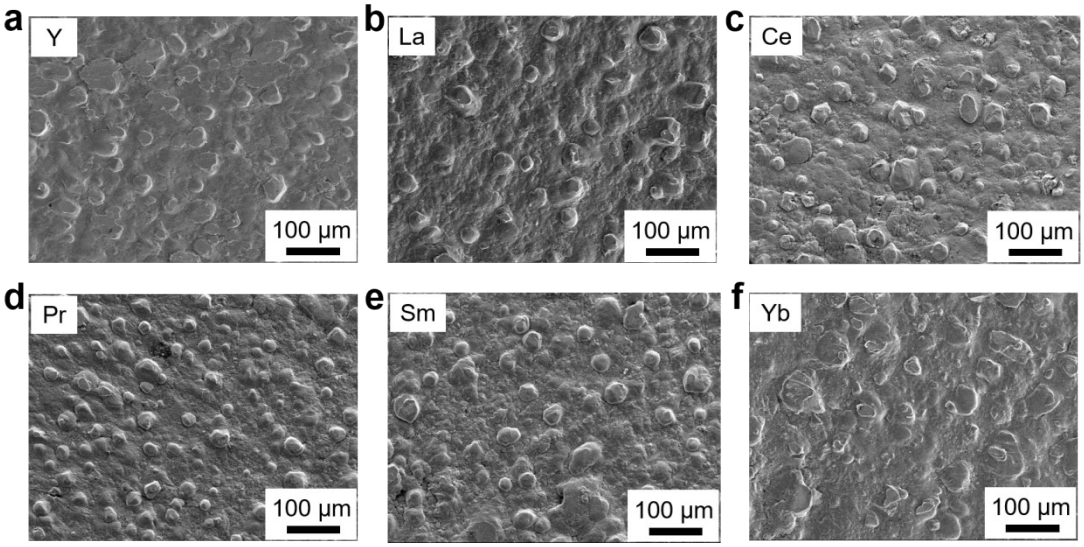

Fig. S11. (a-f) The SEM images of Li-In-RE alloys (RE = Y, La, Ce, Pr, Sm, or Yb).

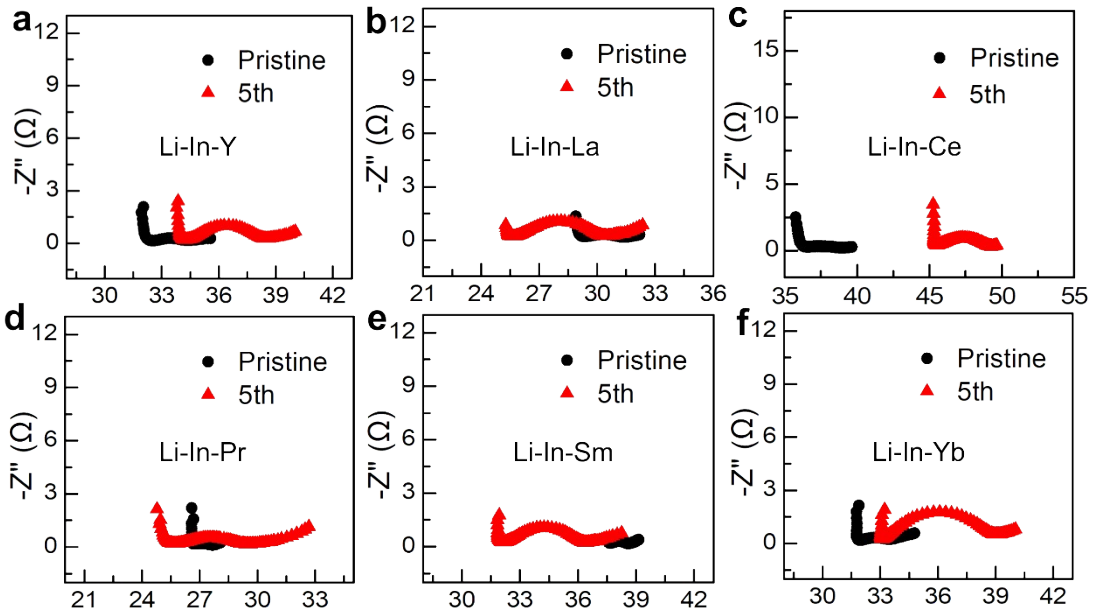

Fig. S12. (a-f) The EIS results of symmetrical solid cells based on Li-In-RE alloys (RE = Y, La, Ce, Pr, Sm, or Yb).

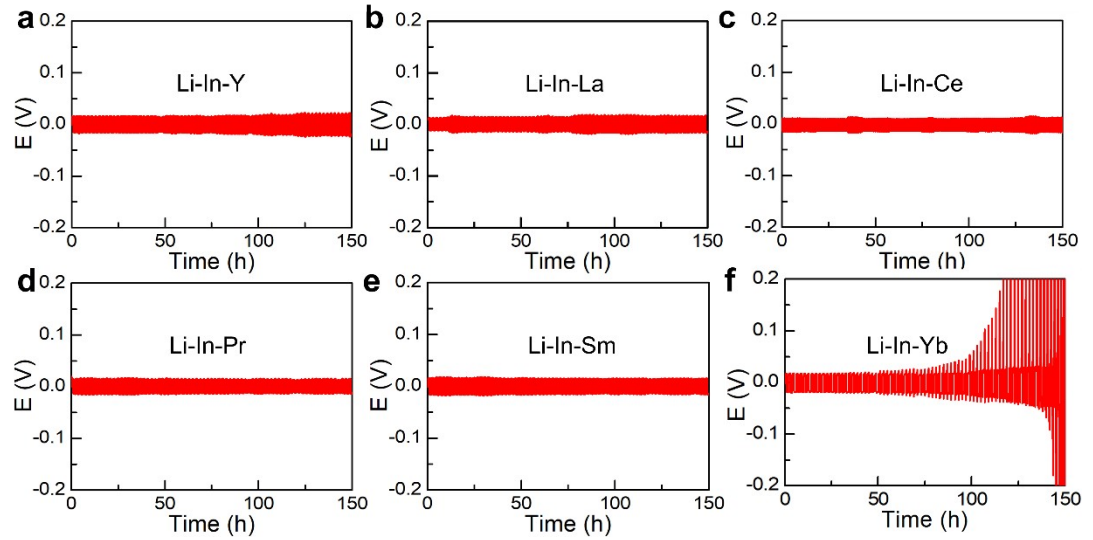

Fig. S13. (a-f) The voltage-time curves of symmetrical solid cells based on Li-In-RE alloys (RE = Y, La, Ce, Pr, Sm, or Yb).

Table S1. The obtained crystal parameters of different phases in Li-In alloy from the XRD Rietveld refinement results.

Phases	In	Li-In
Crystal system	tetragonal	cubic
Space-group	*I* 4/*mmm*	*Fd*-3*m*
Cell parameters	*a* = 3.2541 Å, *b* = 3.2541 Å, *c* = 4.9266 Å, α = *β* = γ = 90.0°	*a* = 6.7600 Å, *b* = 6.7600 Å, *c* = 6.7600 Å, α = *β* = γ = 90.0°
Cell volume	52.169 Å^3	308.91 Å^3

Table S2. The obtained crystal parameters of different phases in Li-In-Ce alloy from the XRD Rietveld refinement results.

Phases	In	Li-In	$CeIn_3$
Crystal system	tetragonal	cubic	cubic
Space-group	*I* 4/*mmm*	*Fd*-3*m*	*Pm*-3*m*
Cell parameters	*a* = 3.2514 Å, *b* = 3.2514 Å, *c* = 4.9193 Å, α = *β* = γ = 90.0°	*a* = 6.7611 Å, *b* = 6.7611 Å, *c* = 6.7611 Å, α = *β* = γ = 90.0°	*a* = 4.6828 Å, *b* = 4.6828 Å, *c* = 4.6828 Å, α = *β* = γ = 90.0°
Cell volume	52.006 $Å^3$	309.07 $Å^3$	102.69 $Å^3$

Table S3. The obtained crystal parameters of different phases in Li-In-Y alloy from the XRD Rietveld refinement results.

Phases	In	Li-In	YIn_3
Crystal system	tetragonal	cubic	cubic
Space-group	*I* 4/*mmm*	*Fd*-3*m*	*Pm*-3*m*
Cell parameters	*a* = 3.2586 Å, *b* = 3.2586 Å, *c* = 4.9321 Å, α = *β* = γ = 90.0°	*a* = 6.7732 Å, *b* = 6.7732 Å, *c* = 6.7732 Å, α = *β* = γ = 90.0°	*a* = 4.5953 Å, *b* = 4.5953 Å, *c* = 4.5953 Å, α = *β* = γ = 90.0°
Cell volume	52.370 $Å^3$	310.73 $Å^3$	97.039 $Å^3$

Table S4. The obtained crystal parameters of different phases in Li-In-La alloy from the XRD Rietveld refinement results.

Phases	In	Li-In	$LaIn_3$
Crystal system	tetragonal	cubic	cubic
Space-group	*I* 4/*mmm*	*Fd*-3*m*	*Pm*-3*m*
Cell parameters	*a* = 3.2559 Å, *b* = 3.2559 Å, *c* = 4.9233 Å, α = *β* = γ = 90.0°	*a* = 6.7700 Å, *b* = 6.7700 Å, *c* = 6.7700 Å, α = *β* = γ = 90.0°	*a* = 4.7407 Å, *b* = 4.7407 Å, *c* = 4.7407 Å, α = *β* = γ = 90.0°
Cell volume	52.192 $Å^3$	310.29 $Å^3$	106.54 $Å^3$

Table S5. The obtained crystal parameters of different phases in Li-In-Pr alloy from the XRD Rietveld refinement results.

Phases	In	Li-In	$PrIn_3$
Crystal system	tetragonal	cubic	cubic
Space-group	*I* 4/*mmm*	*Fd*-3*m*	*Pm*-3*m*
Cell parameters	*a* = 3.2520 Å, *b* = 3.2520 Å, *c* = 4.9323 Å, α = *β* = γ = 90.0°	*a* = 6.7714 Å, *b* = 6.7714 Å, *c* = 6.7714 Å, α = *β* = γ = 90.0°	*a* = 4.6708 Å, *b* = 4.6708 Å, *c* = 4.6708 Å, α = *β* = γ = 90.0°
Cell volume	52.163 $Å^3$	310.49 $Å^3$	101.90 $Å^3$

Table S6. The obtained crystal parameters of different phases in Li-In-Sm alloy from the XRD Rietveld refinement results.

Phases	In	Li-In	$SmIn_3$
Crystal system	tetragonal	cubic	cubic
Space-group	*I* 4/*mmm*	*Fd*-3*m*	*Pm*-3*m*
Cell parameters	*a* = 3.2565 Å, *b* = 3.2565 Å, *c* = 4.9290 Å, α = *β* = γ = 90.0°	*a* = 6.7715 Å, *b* = 6.7715 Å, *c* = 6.7715 Å, α = *β* = γ = 90.0°	*a* = 4.6258 Å, *b* = 4.6258 Å, *c* = 4.6258 Å, α = *β* = γ = 90.0°
Cell volume	52.270 $Å^3$	310.50 $Å^3$	98.983 $Å^3$

Table S7. The obtained crystal parameters of different phases in Li-In-Yb alloy from the XRD Rietveld refinement results.

Phases	In	Li-In	$YbIn_3$
Crystal system	tetragonal	cubic	cubic
Space-group	*I* 4/*mmm*	*Fd*-3*m*	*Pm*-3*m*
Cell parameters	*a* = 3.2565 Å, *b* = 3.2565 Å, *c* = 4.9291 Å, α = *β* = γ = 90.0°	*a* = 6.7722 Å, *b* = 6.7722 Å, *c* = 6.7722 Å, α = *β* = γ = 90.0°	*a* = 4.5902 Å, *b* = 4.5902 Å, *c* = 4.5902 Å, α = *β* = γ = 90.0°
Cell volume	52.272 $Å^3$	310.59 $Å^3$	96.720 $Å^3$

REFERENCES

1. Shi, X.; Zeng, Z.; Zhang, H.; Huang, B.; Sun, M.; Wong, H. H.; Lu, Q.; Luo, W.; Huang, Y.; Du, Y. Gram-scale synthesis of nanosized Li_3HoBr_6 solid electrolyte for all-solid-state Li–Se battery. *Small Methods* **2021**, 2101002.
2. Toby, B. EXPGUI, a graphical user interface for GSAS. *J. Appl. Crystallogr.* **2001**, *34* (2), 210-213.
3. Kresse, G.; Furthmüller, J. Efficiency of ab-initio total energy calculations for metals and semiconductors using a plane-wave basis set. *Comput. Mater. Sci* **1996**, *6* (1), 15-50.
4. Kresse, G.; Hafner, J. Ab initio molecular dynamics for liquid metals. *Phys. Rev. B* **1993**, *47* (1), 558-561.
5. Kresse, G.; Joubert, D. From ultrasoft pseudopotentials to the projector augmented-wave method. *Phys. Rev. B* **1999**, *59* (3), 1758-1775.
6. Sydor, M.; Pinkowski, G.; Jasińska, A. The brinell method for determining hardness of wood flooring materials. *Forests* **2020**, *11* (8), 878.
7. Wan, T.H.; Saccoccio, M.; Chen, C.; Ciucci, F. Influence of the discretization methods on the distribution of relaxation times deconvolution: Implementing radial basis functions with DRT tools, *Electrochim. Acta* **2015**, *184*, 483-499.